# PROCESSING OF SOFC ANODES FOR IMPROVED INTERMEDIATE TEMPERATURE CATALYTIC ACTIVITY AT HIGH FUEL UTILIZATION

Yanchen Lu, Paul Gasper, Uday Pal,
Srikanth Gopalan and Soumendra Basu

Division of Materials Science and Engineering
Boston University

*Presented at the 17th Annual Solid Oxide Fuel Cell (SOFC) Project Review Meeting, July 19-21, 2016, Pittsburgh, PA.*

# Motivations for Anode Infiltration

- Performance enhancement
- Ni reduction
- Incorporation of alternate materials for
  - Sulfur tolerance
  - Coking tolerance
- High fuel utilization tolerance

# Does Fuel Utilization Affect Anodic Losses?

- In a real stack, fuel utilization can exceed 85%
- This effect is replicated by controlling the $H_2$-$H_2O$ gas mix at the anode.

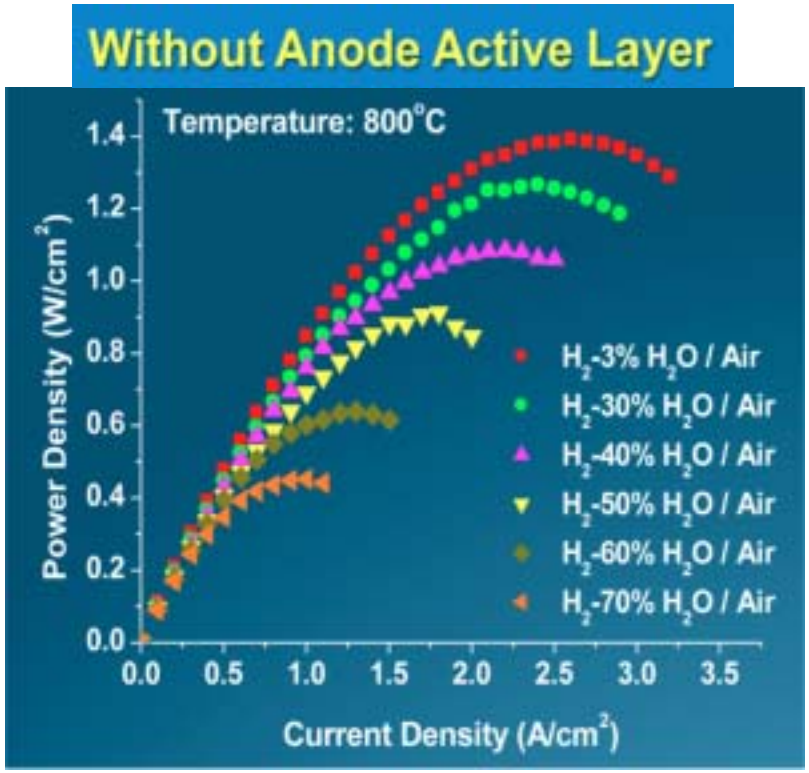


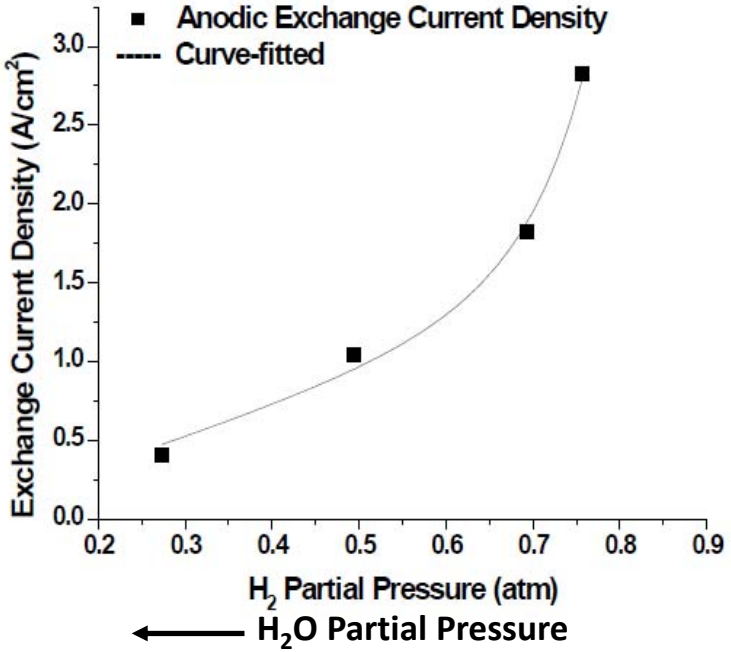


*Yoon et al., J. Electrochem. Soc.,* ***155****, 2008, pp B610*

- Increasing fuel utilization can seriously degrade cell performance
- Effect will be even more exaggerated at lower temperatures

# Effect of TPB Length

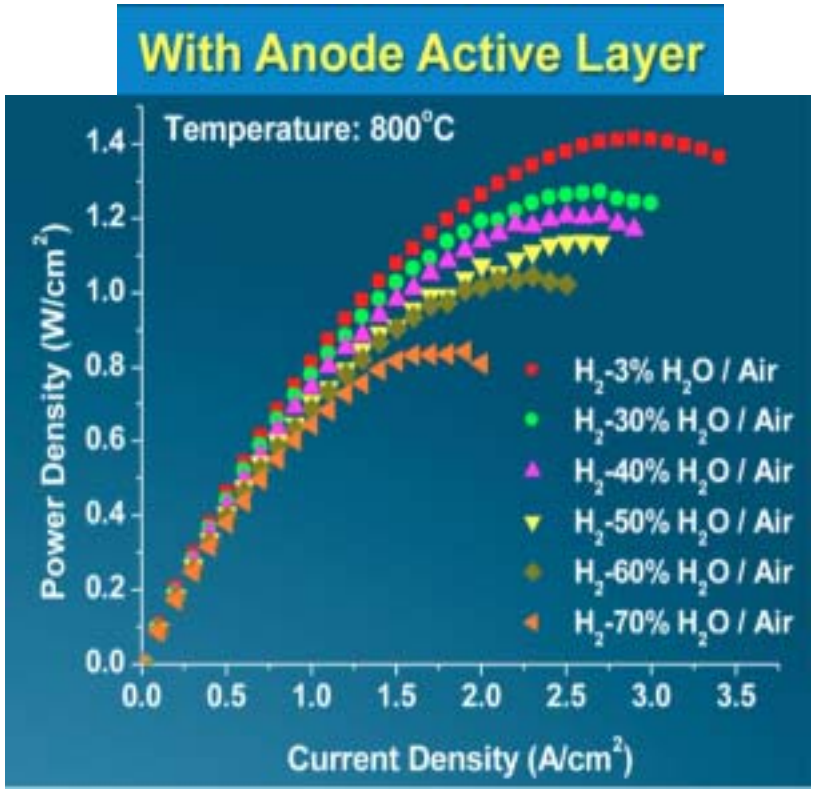


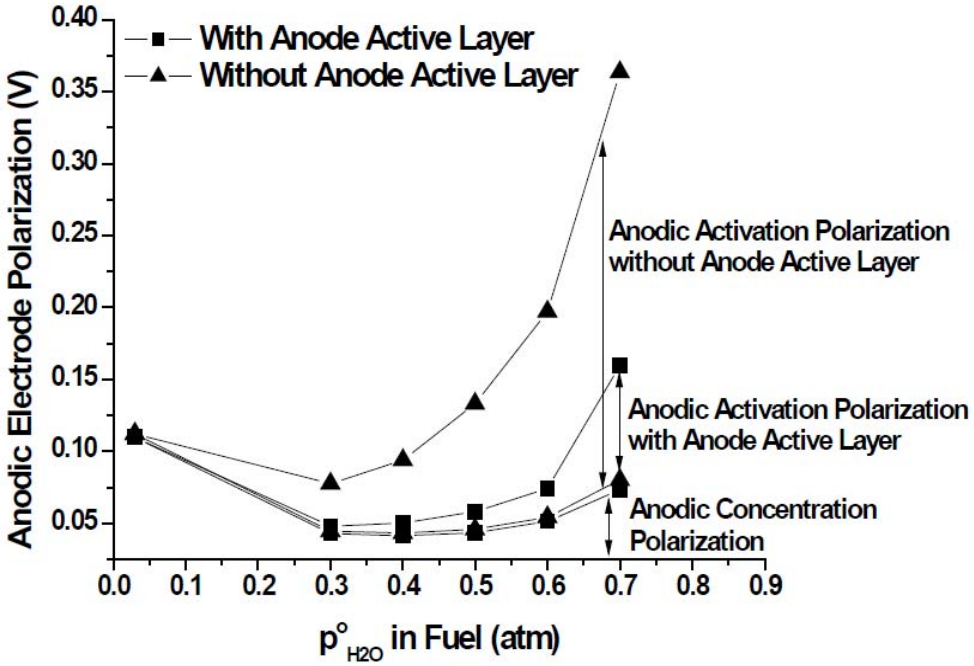


Current density fixed at 1.5 A/cm$^2$

*Yoon et al., J. Electrochem. Soc.,* ***155****, 2008, pp B610*

Increasing TPB length improves performance and alleviates the high fuel utilization related performance degradation

# Characterization of TPB Lengths

| Title | Group | Technique | TPB Length ($\mu m/\mu m^3$) |
|---|---|---|---|
| Quantification of SOFC anode microstructure based on dual beam FIB-SEM technique (2011) | Yoshida | FIB-SEM | 2.37-2.49 |
| Three-dimensional reconstruction and analysis of an entire solid oxide fuel cell by full-field transmission X-ray microscopy (2013) | Barnett | Nano-TXM | 3.06 (Total)<br>2.89 (Active) |

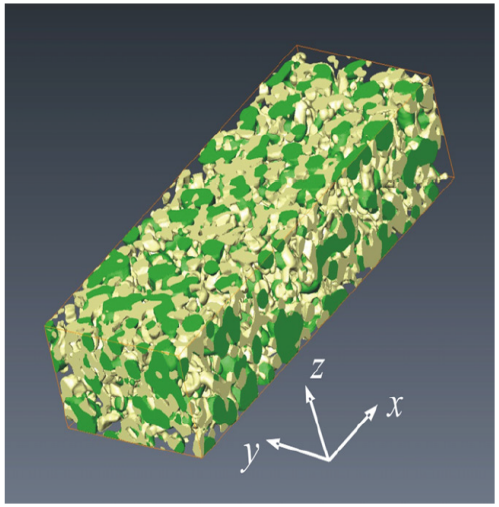


FIB-SEM (Awai et al. 2011)

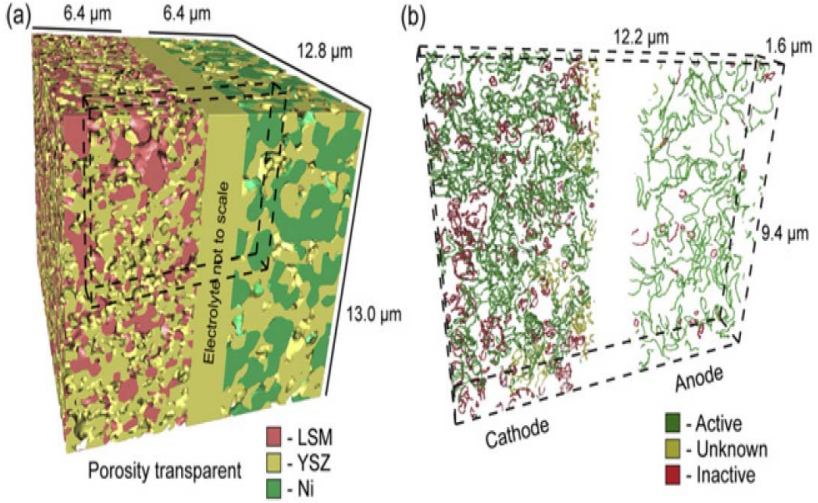


Nano-TXM (Cronin et al. 2013)

Typical TPB length in SOFC anodes is ~ 3 $\mu m/\mu m^3$

# Summary of Anode Liquid Infiltration Studies

| Group | Year | Infiltrate | Substrate | Reference |
|---|---|---|---|---|
| Atkinson | 2008 | 0.3 M solution of $Ni(NO_3)_2$ ·6H2O in ethanol | Porous YSZ | Busawon, A. N., 2008, Electrochemical and Solid-State Letters 11 (10), B186-B189. |
| Klemensø | 2010 | $Ni(NO_3)_2 \cdot 6H_2O$ and CGO | Porous YSZ | Klemenso, T., 2010, J. Power Sources 195, 7295-7301. |
| Gorte | 2011 | Tungsten bronzes with Pd catalyst | Porous YSZ | Adijanto, L., 2011, Int. J. of Hydrogen Energy 36, 15722-15730. |
| Buyukaksoy | 2012 | polymeric NiO precursor | Porous YSZ | Buyukaksoy, A., 2012, J. Electrochemical Society 159 (12), F841-F848 |
| Hanifi | 2014 | LSM and SDC | Porous YSZ | Hanifi, A., 2014, J. Power Sources 266, 121-131. |
| Keyvanfar | 2014 | $Ni(NO_3)_2$ with Triton-X, urea | Porous YSZ | Keyvanfar, P., 2014, J. Electrochemical Society 161 (5), F660-F667. |
| Barnett | 2015 | $Ni(NO_3)_2$ precursor | Porous LSGM | https://www.krellinst.org/nnsassgf/conf/2015/pres/miller2010.pdf. |
| Liu | 2014 | BZCYYb solution | Ni-YSZ | Sengodan, S., 2014, J. Electrochemical Society 161 (5), F668-F673. |

# Infiltrating Percolating Ni/YSZ Cermets

- Ni infiltration of Ni/YSZ cermets is not widely explored
- Conventional Ni/YSZ anodes are already percolating
- Only infiltrated Ni particles on YSZ will add to TPB length
- Additional TPB will help retain performance at high $P(H_2O)$

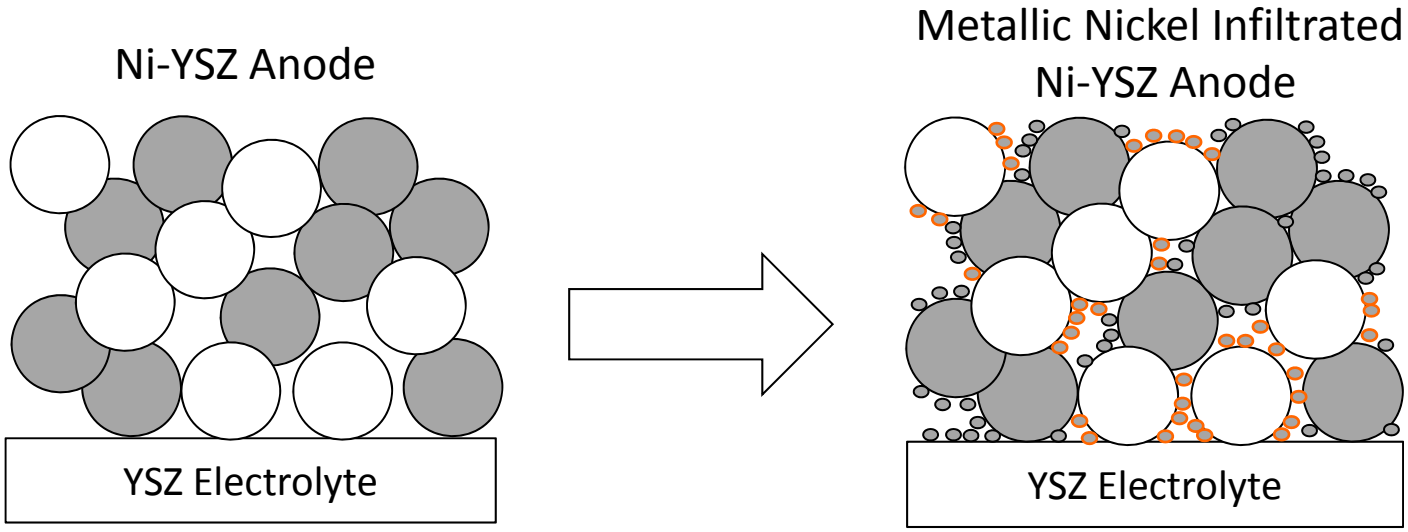

# Characterization of MSRI Button Cells

SEM

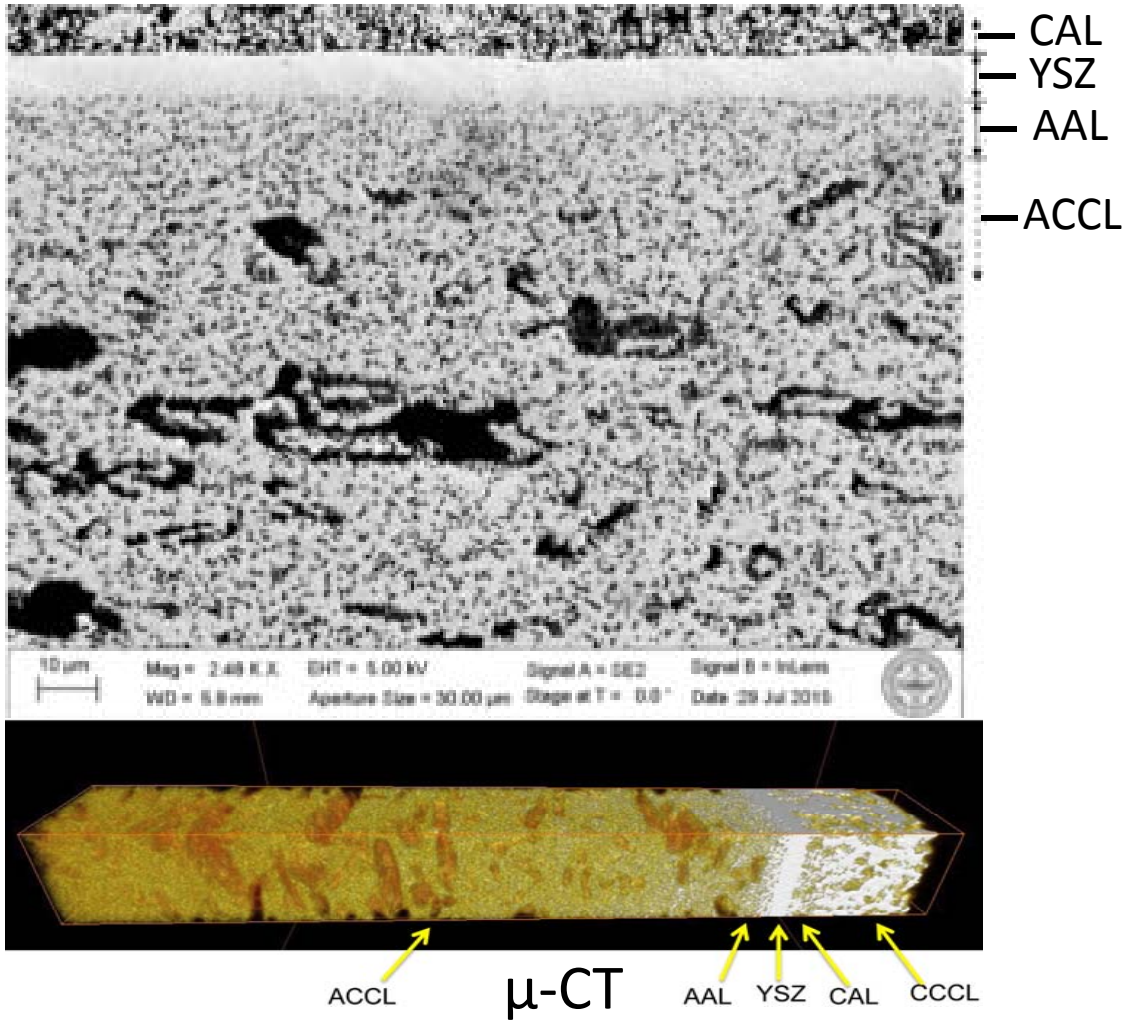


μ-CT

FIB-SEM- AAL

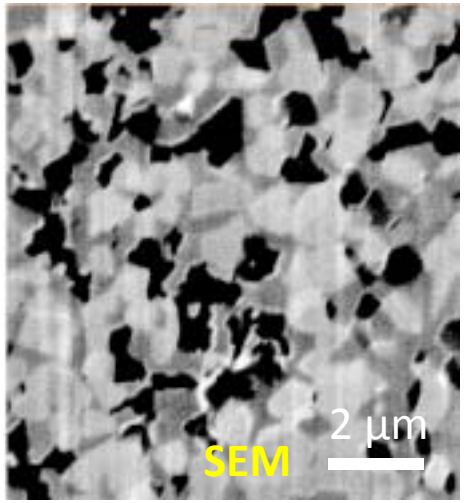


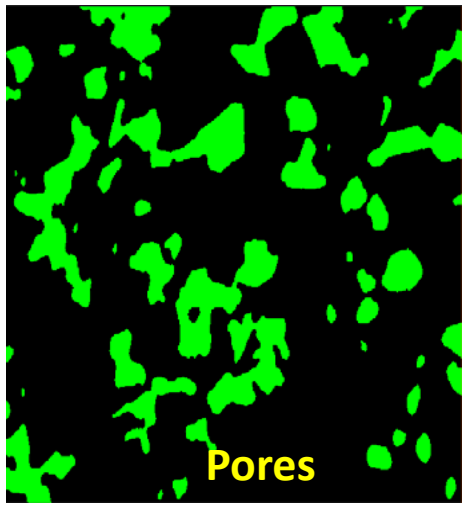


Porosity in reduced cell ~ 35%

Surface area of large pores ($D_{eff}$>3μm) ~ 0.22 $\mu m^2/\mu m^3$ of anode

# Liquid Infiltration of Ni-YSZ Anodes

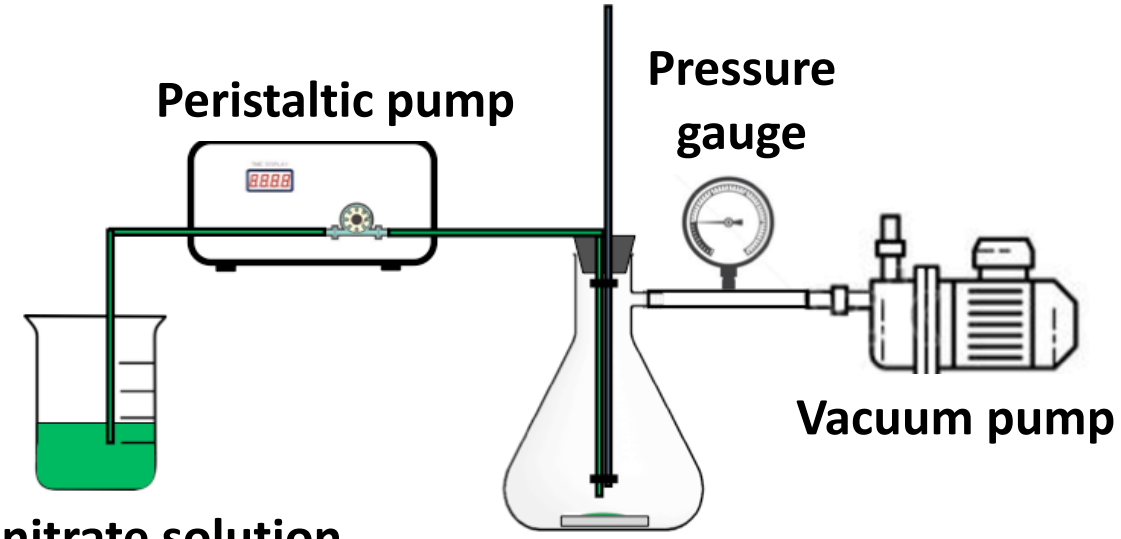


Button cell from MRSI

Reduce cell (800° C, 2 hours 5% $H_2$)

Weigh cell

N cycles

Liquid infiltration in vacuum (<10 mbar)

Dry in air (100° C, 20 min), decompose nitrates to NiO in air (320° C, 20 min)

Reduce cell (800° C, 2 hours 5% $H_2$)

Characterization (SEM, FIB, TEM)

# Results of Liquid Infiltration

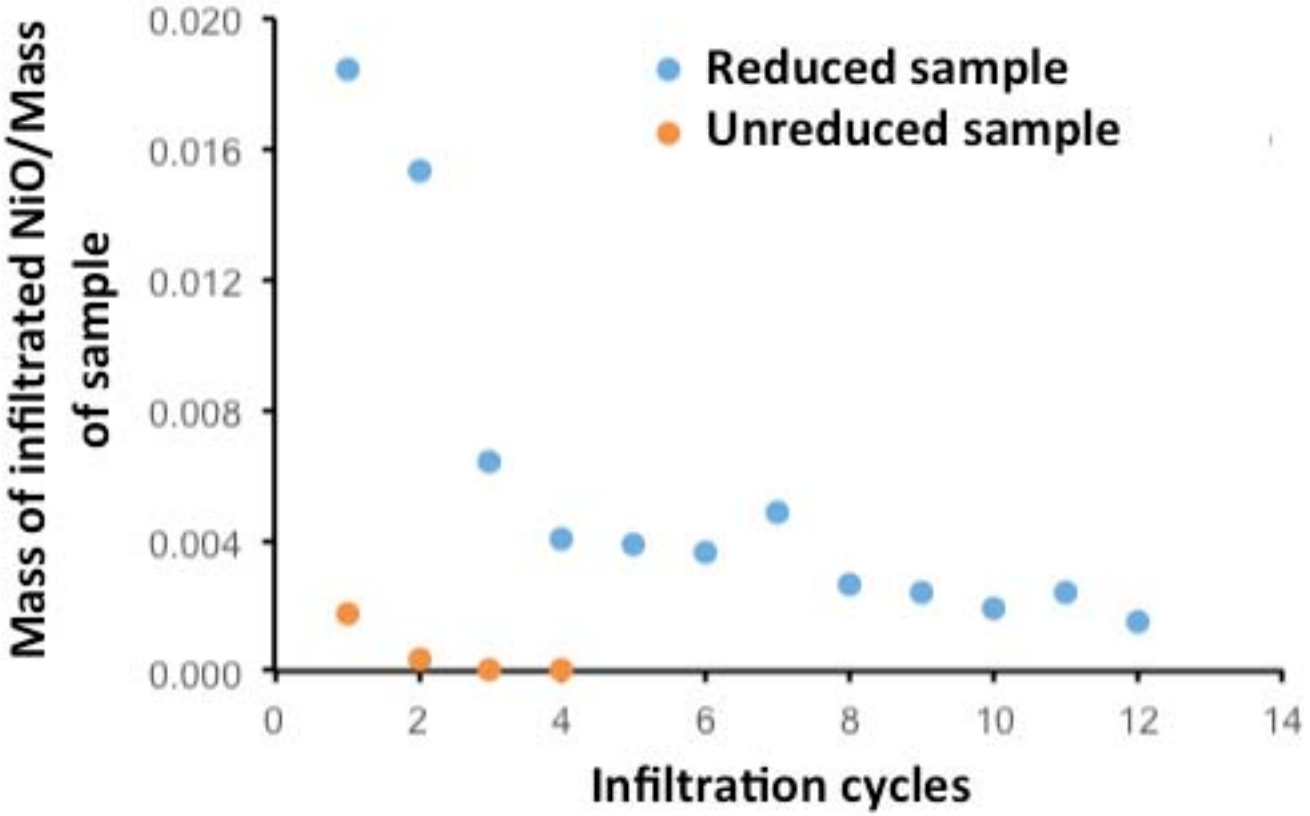


For the reduced sample, after 12 cycles, the infiltrated Ni content corresponds to:

- 2.35 volume % of anode, or:
- 6.75 volume % of the pores

# Characterization of Infiltrated Anodes

Reduced sample before infiltration

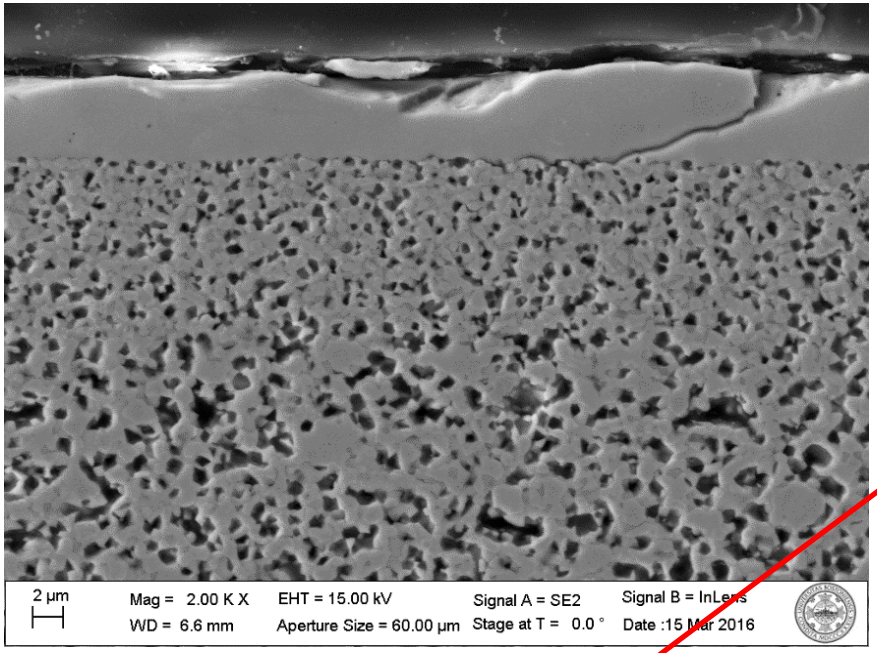


After-infiltration and reduction

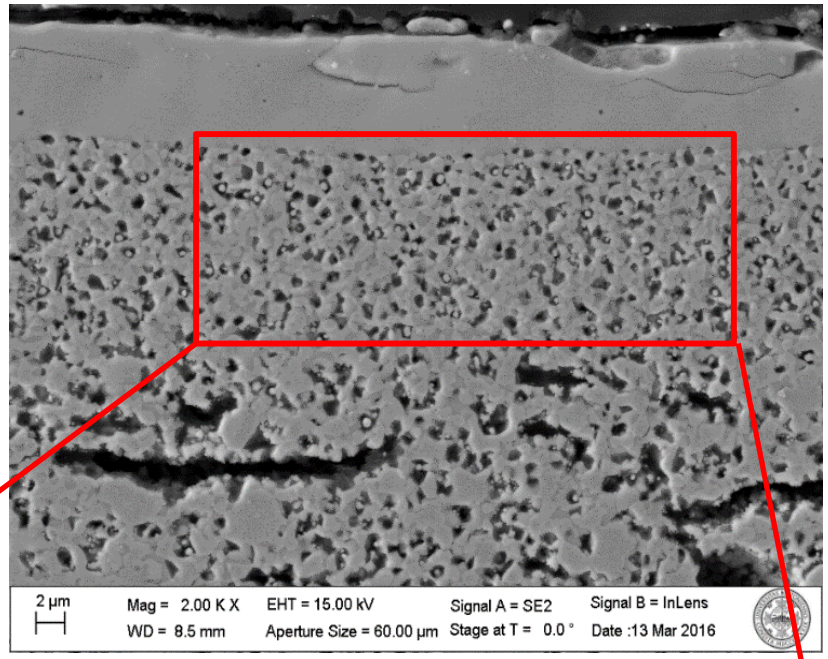


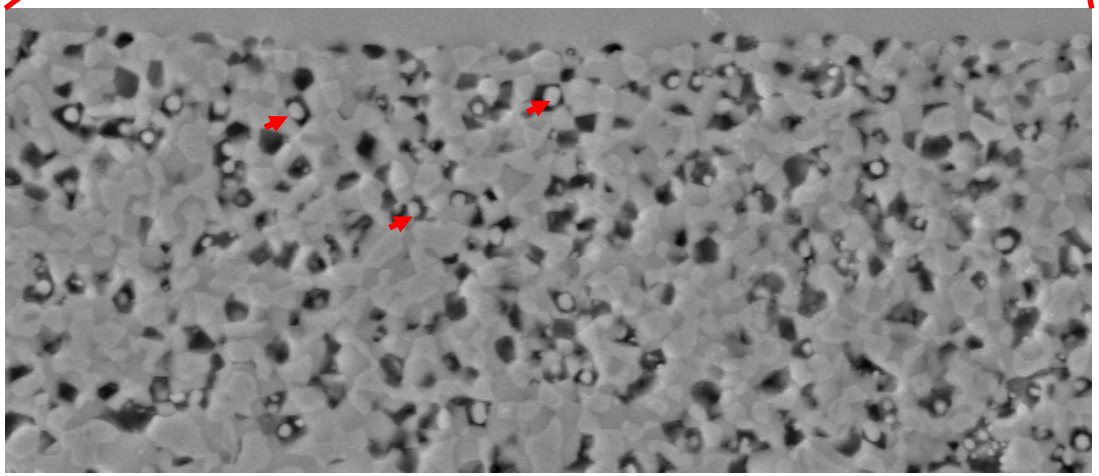

Liquid infiltration of conventional Ni/YSZ cermet can can lead to deposition in the anode active layer

# Characterization of Infiltrated Anodes

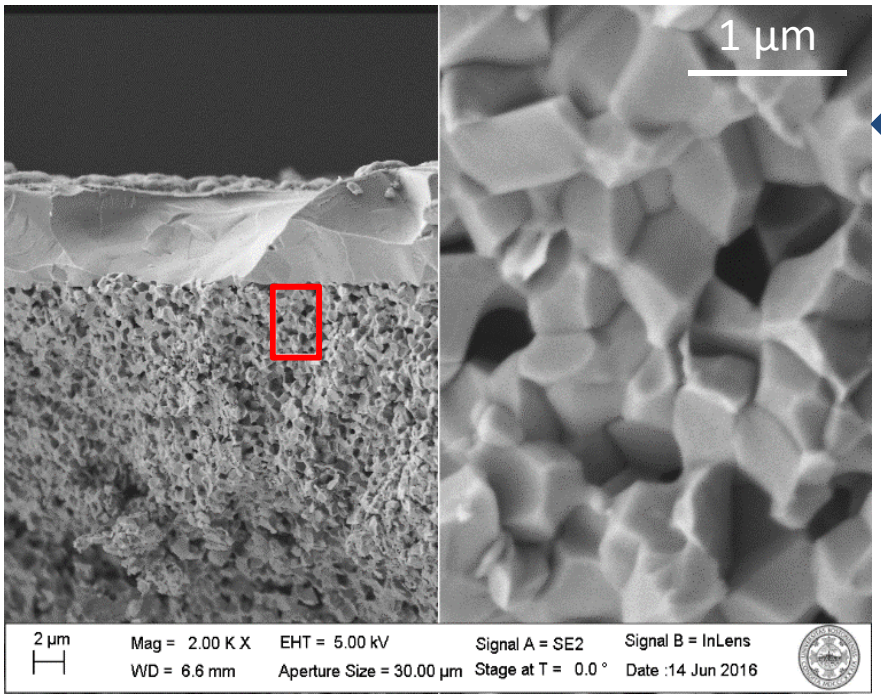


SEM of fractured cross-section (pre-infiltration)

SEM of fractured cross-section (post-infiltration and reduction)

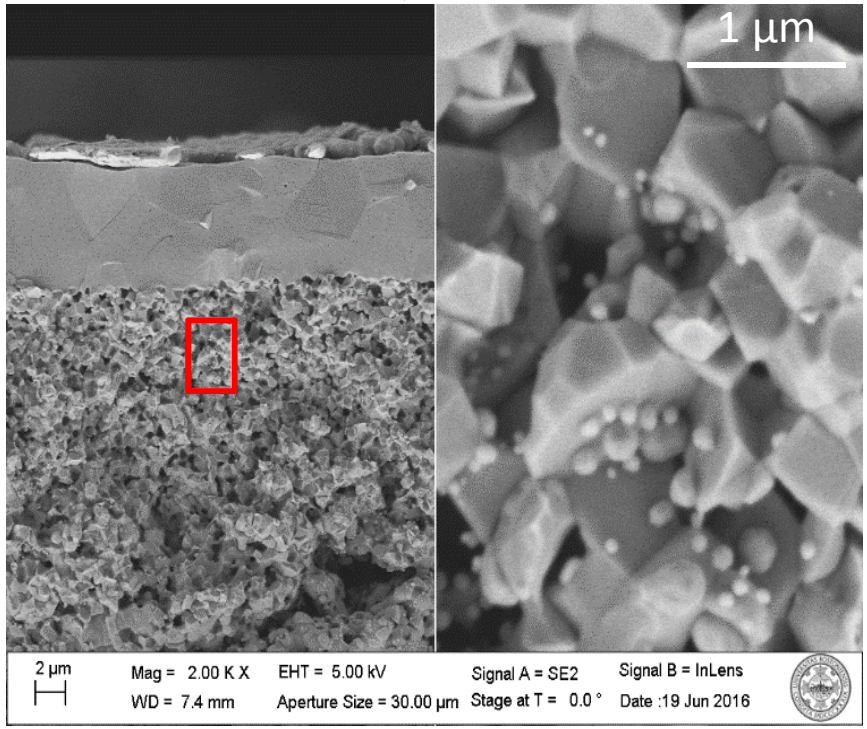


Particle size distributions in the i) anode active layer, ii) anode current collector and iii) areas around large pores were measured and analyzed

# Quantification of Particle Diameters

SEM Image | Ni Particle selection | Image separation | $D_{eff}$ calculation

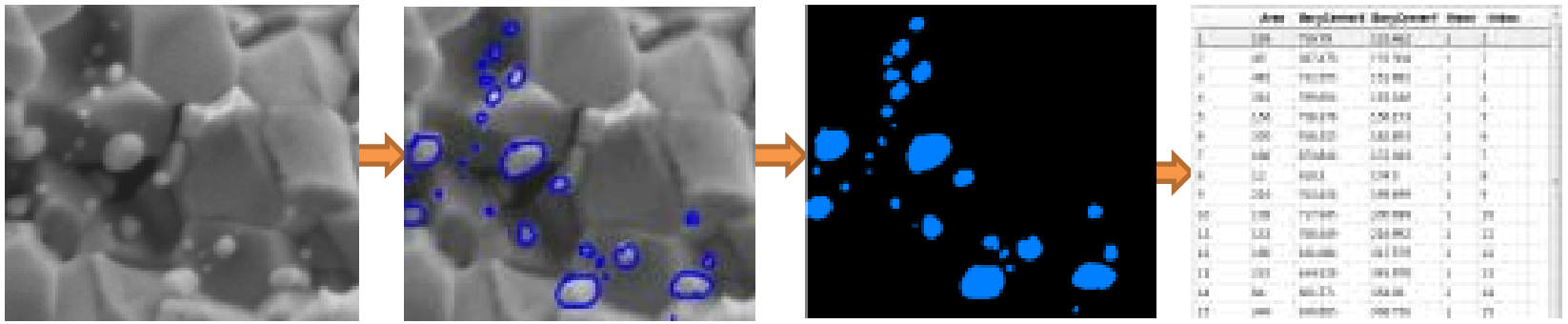

Particle Size Distribution in Active Layer

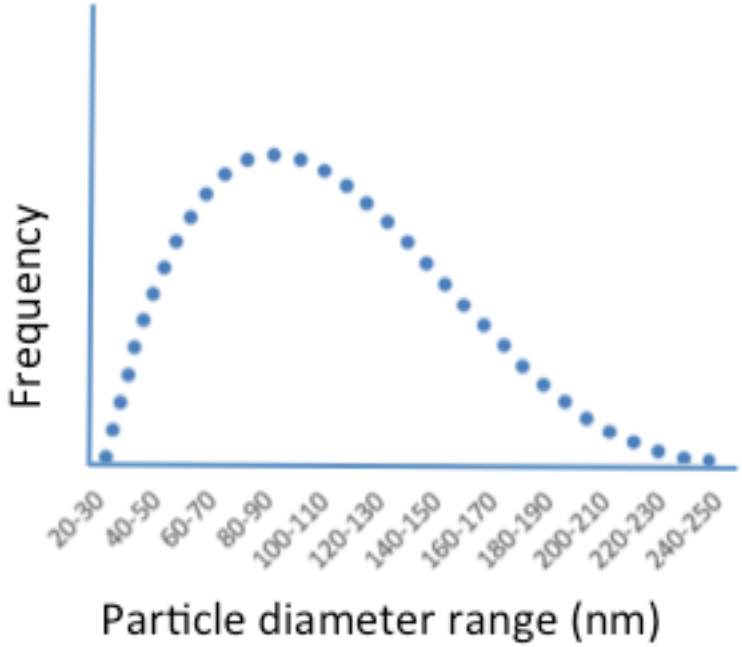


Particle size distribution and density gives additional TBP length as a function of position in the infiltrated anode

# Location of Ni Precipitate Nucleation

Phase determination by EDX on fracture cross-sections

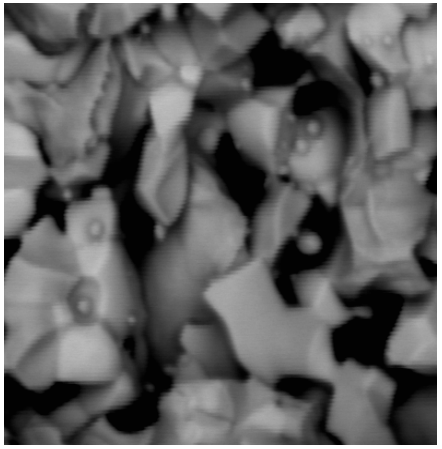

SE Map

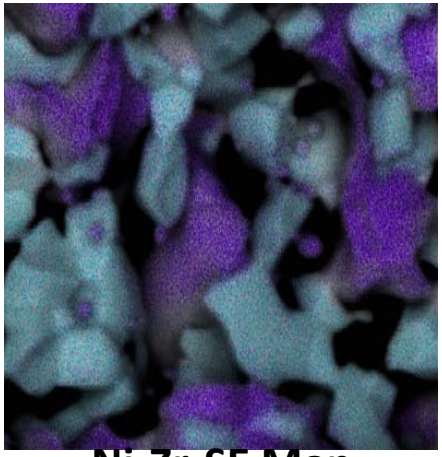

Ni-Zr-SE Map

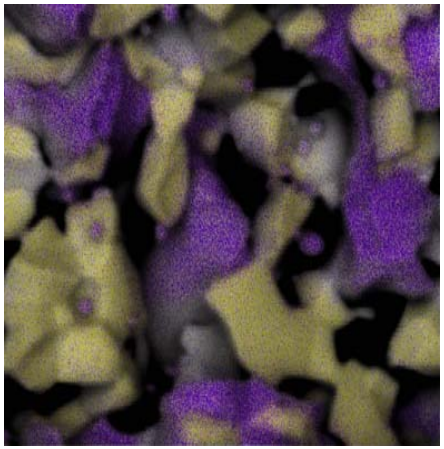

Ni-O-SE Map

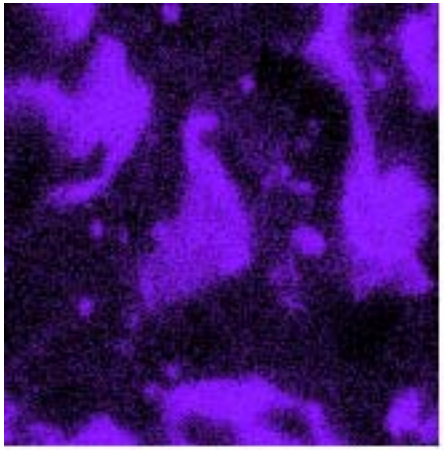

Ni Map

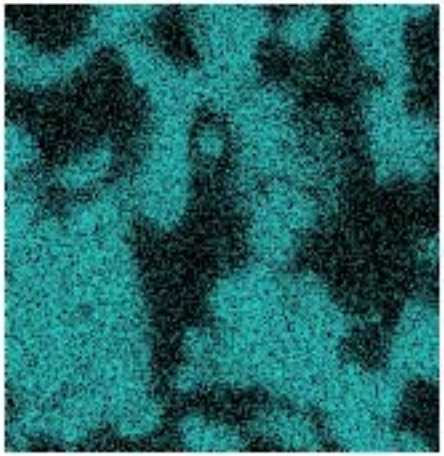

Zr Map

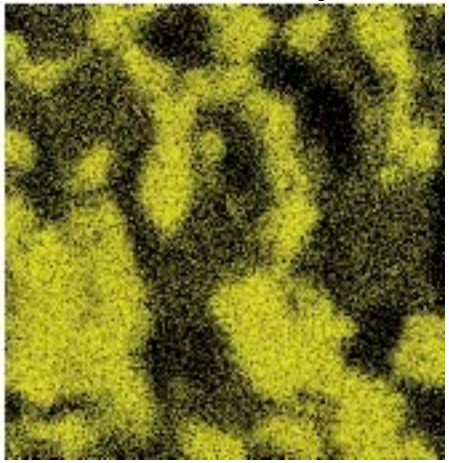

O Map

- Ni particles tend to strongly favor YSZ grains
- Most Ni particles will contribute to TPB formation

# Additional TPB due to Liquid Infiltration

| Region of Interest | Average Particle Size (nm) | Additional TPB length ($\mu m/\mu m^3$) |
|---|---|---|
| Active Layer | 112 | 5.46 |
| Current collecting layer (not including large pores) | 113 | 4.63 |
| Region around large pores | 106 | 9.26 |

Infiltration of standard Ni/YSZ anode more than doubles TPB length

# Challenges of Liquid Infiltration

- Time consuming procedure
- Thermal cycling introduces possibility of electrolyte failure
- Maintaining cell integrity in reduced state during processing steps and electrochemical testing is challenging

**Alternate approach**:

Vapor phase infiltration of metallic Ni into anode using water vapor and forming gas

# Thermodynamics of Ni Vaporization: Effect of T

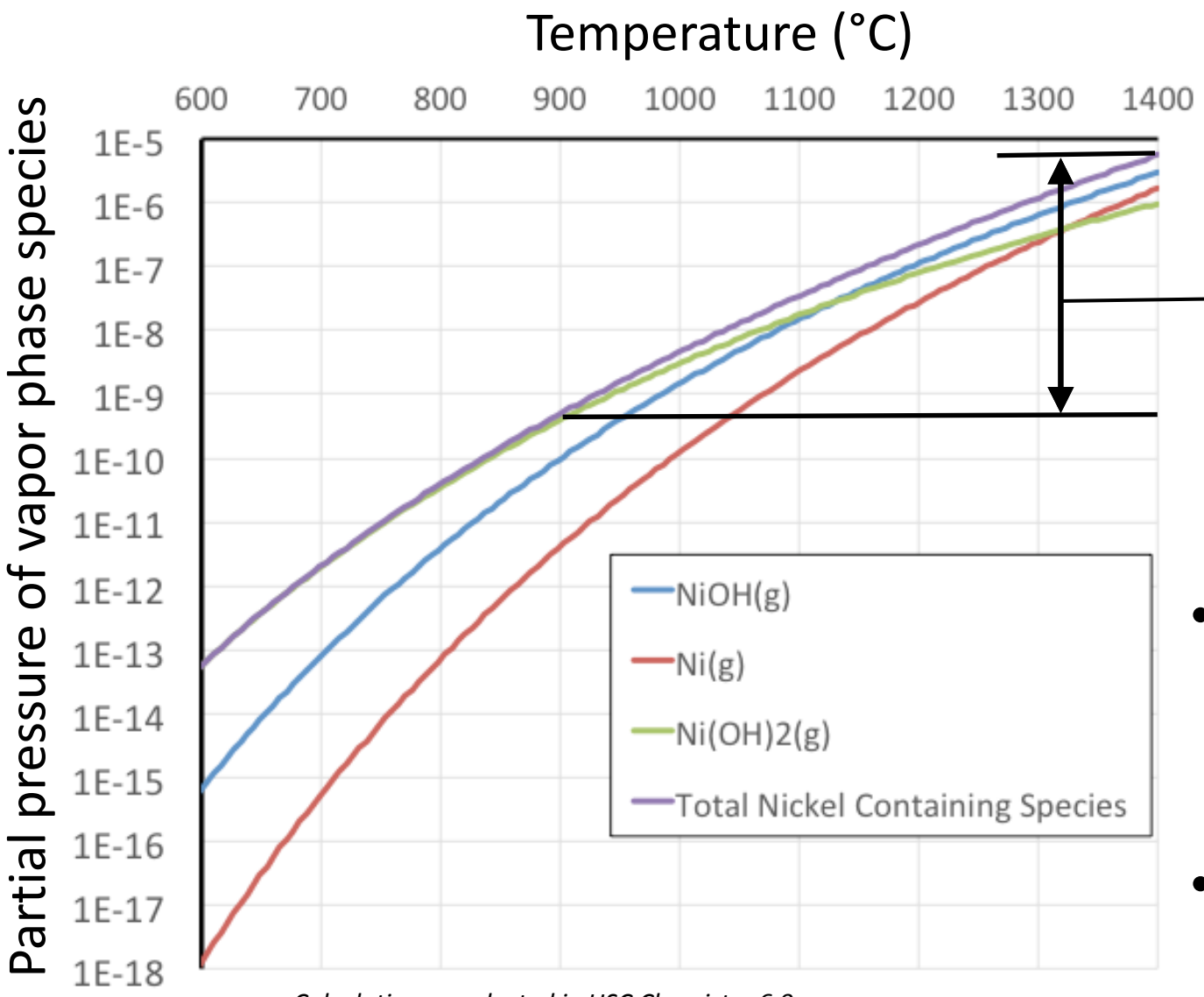


~ $10^4$ reduction in equilibrium partial pressure of Ni-containing vapor species on cooling from 1400°C-900°C

*Calculations conducted in HSC Chemistry 6.0.*

- 75% Forming gas (5% $H_2$, 95% Ar)/25% water vapor
- Unlimited Ni supply

# Thermodynamics of Ni Vaporization: $p(H_2O)$

- X% water vapor/(100-X)% forming gas (5% $H_2$, 95% Ar)
- Unlimited Ni supply
- 1400°C

Hertz-Knudsen equation shows that only a small surface is needed to reach thermodynamic Ni vapor partial pressure

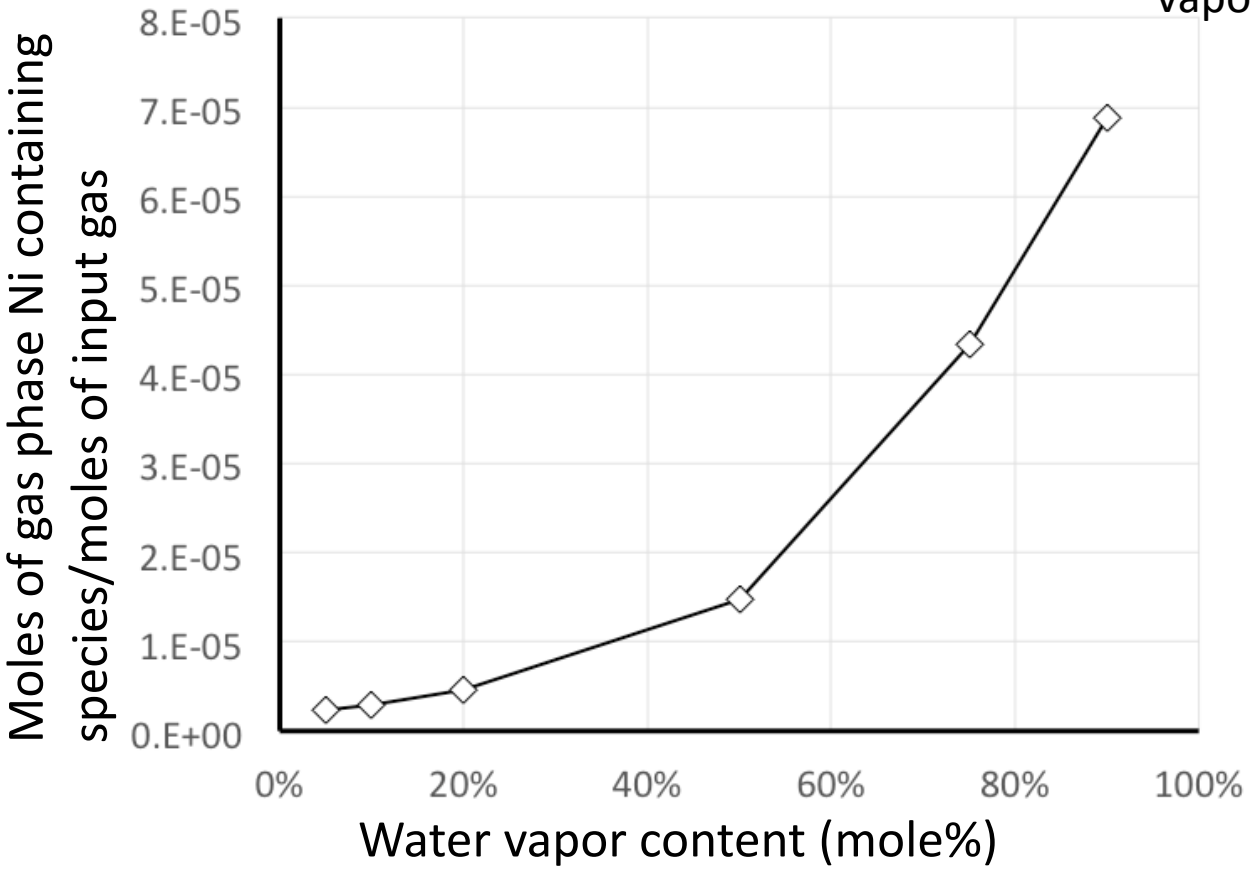


| Nickel Vaporization Rate (1000 ccm gas flow rate) | |
|---|---|
| **Water vapor content** | **Grams nickel per minute** |
| 5% | 5.92E-06 |
| 10% | 7.66E-06 |
| 20% | 1.20E-05 |
| 50% | 3.89E-05 |
| 75% | 1.13E-04 |
| 90% | 1.80E-04 |

~ 30X

*Calculations conducted in HSC Chemistry 6.0.*

# Thermodynamics of Ni Vaporization: $P_{tot}$

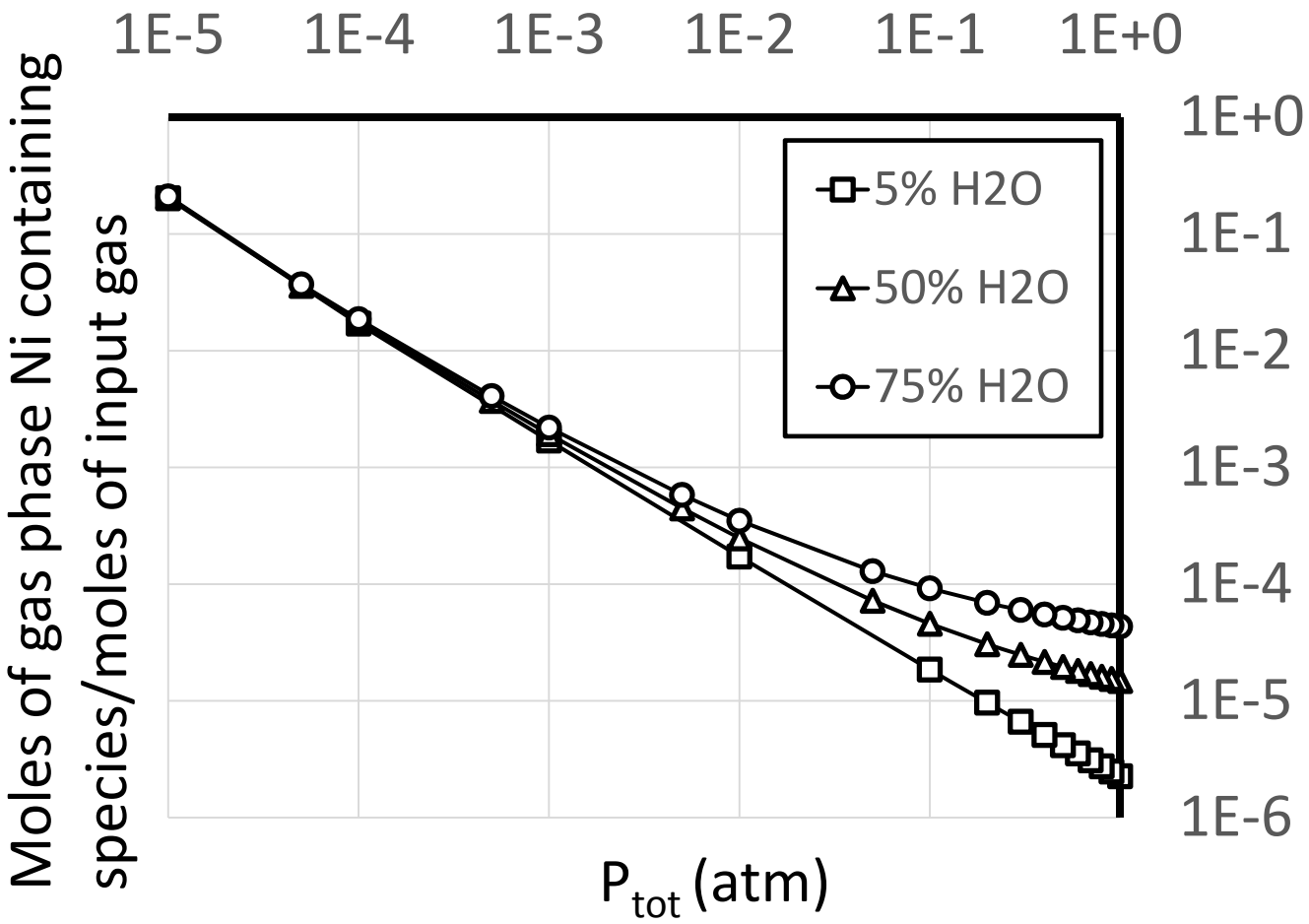


| Nickel Vaporization Rate (1000 ccm gas flow rate, 5% $H_2O$) | |
|---|---|
| **Pressure (bar)** | **grams nickel per minute** |
| 1 | 5.92E-06 |
| 0.01 | 4.52E-04 |
| 0.001 | 4.45E-03 |
| 0.0001 | 4.47E-02 |
| 0.00001 | 5.30E-01 |

- X% water vapor/ (100-X)% forming gas (5% $H_2$, 95% Ar)
- Unlimited Ni supply
- 1400°C

*Calculations conducted in HSC Chemistry 6.0.*

# Thermodynamics of Ni Vaporization: $P_{tot}$

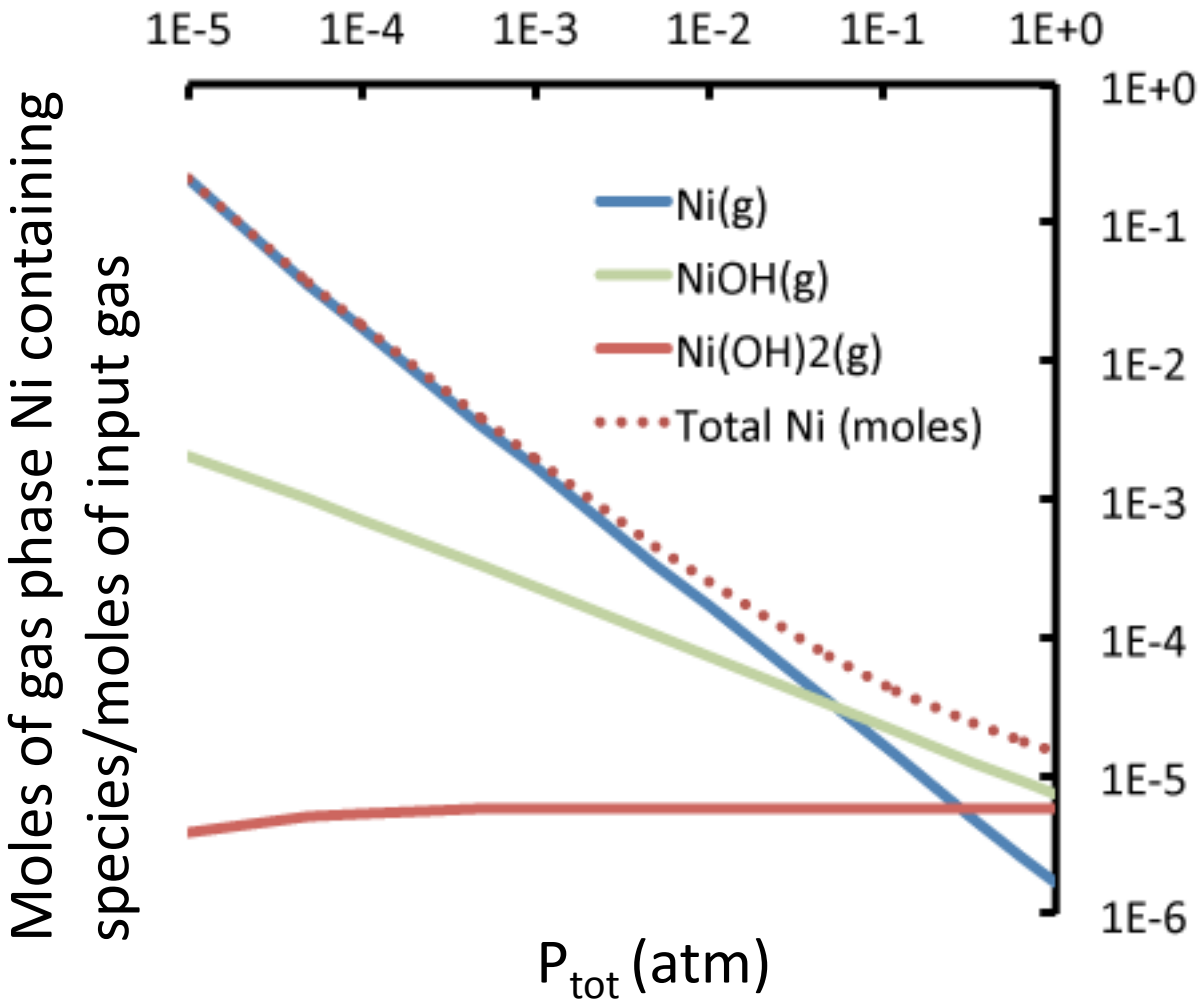


- 50% water vapor/ 50% forming gas (5% $H_2$, 95% Ar)
- Unlimited Ni supply
- 1400°C

Since at low $P_{tot}$, Ni(g) species dominates, water vapor may not be needed

# Experimental Validation of Ni Vaporization

- 1400°C furnace
- Flowing forming gas and water vapor
- One-stage vacuum pump for low pressure experiments

| 1400°C, 0.05 moles/min gas flow | Theoretical Evaporation (gm/hr) | Experimental Evaporation (gm/hr) | Ratio of Actual/Expected |
|---|---|---|---|
| **5% $H_2O$, 1 atm** | 3.55E-04 | 3.0E-04 | **85%** |
| **10% $H_2O$, 1 atm** | 5.15E-04 | 4.3E-04 | **83%** |
| **75% $H_2O$, 1 atm** | 7.60E-03 | 4.7E-03 | **62%** |
| **5% $H_2O$, 0.1 atm** | 2.91E-03 | 1.6E-03 | **55%** |
| **75% $H_2O$, 0.1 atm** | 1.45E-02 | 9.6E-03 | **66%** |

| Normalized amount of nickel evaporated | 1 atm | Vacuum Pump (~0.1 atm with gas flow) |
|---|---|---|
| **5% $H_2O$** | 1 | 5.3X |
| **75% $H_2O$** | 15.7X | 32X |

# Feasibility of Vapor Deposition of Nickel

Deposition outside of $ZrO_2$ tube

Ni source at 1400°C, deposit location shown at 900°C

10% water vapor/90% forming gas

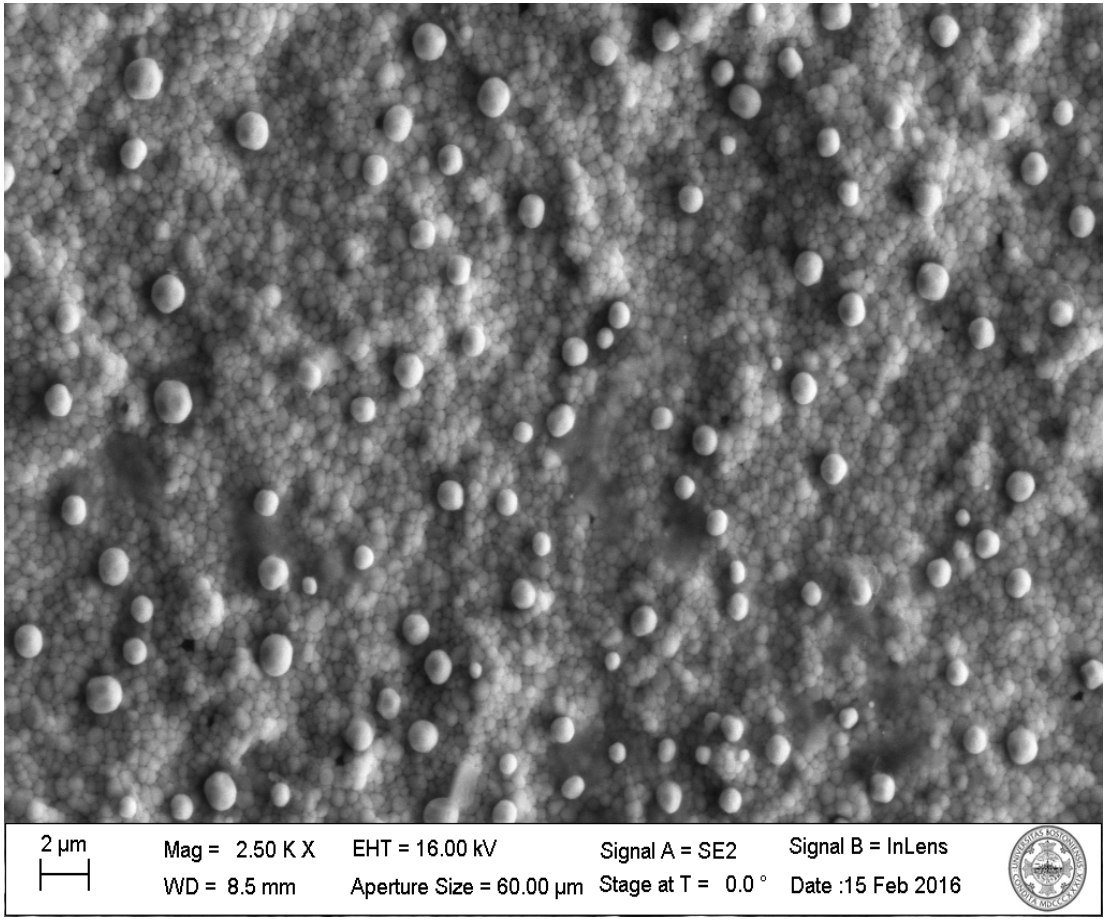

# Single Step Deposition and Testing

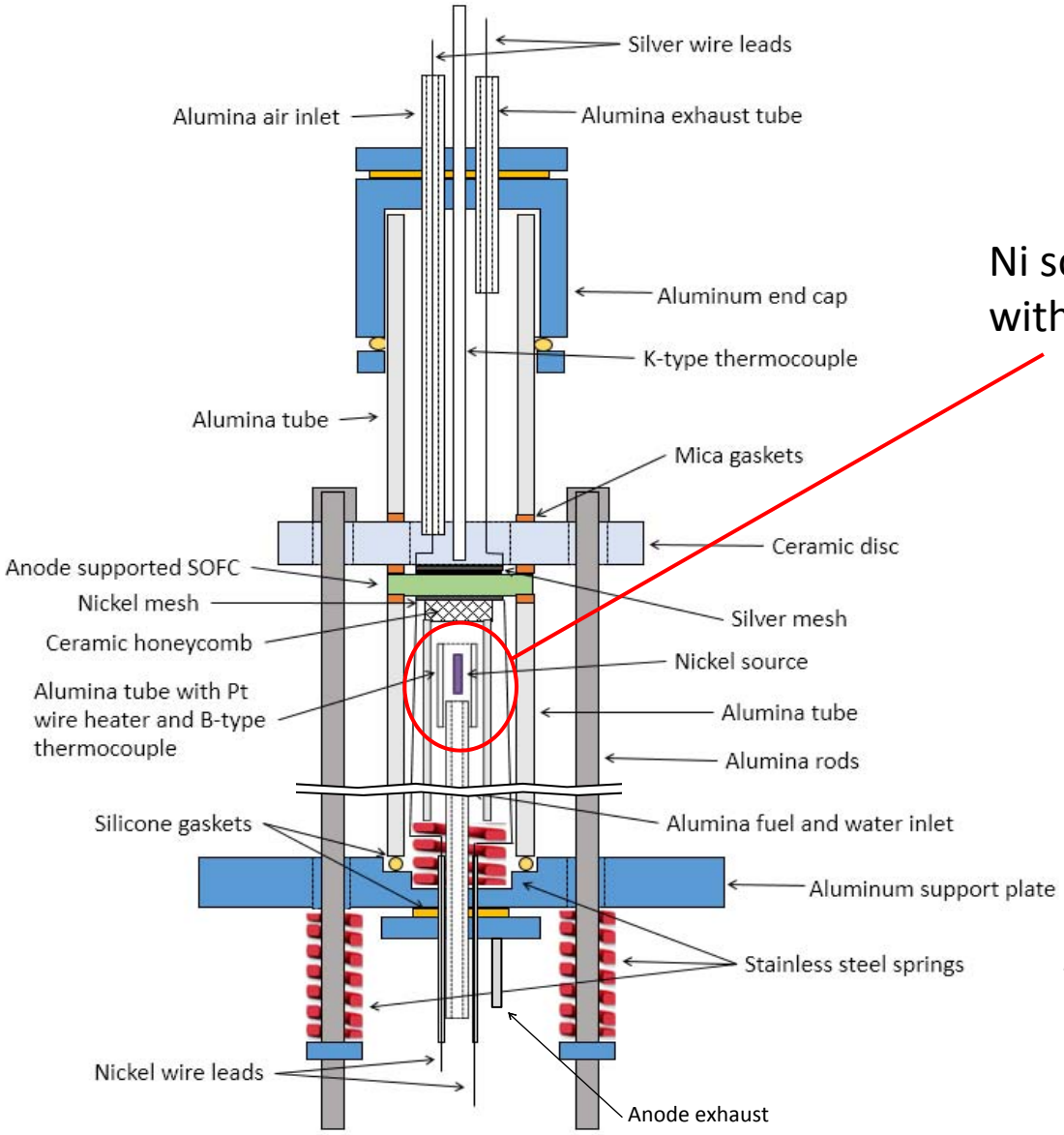


Ni source and heater with adjustable position

*Patent disclosure filed with BU Office of Technology Development*

# *In-Situ* Vapor Phase Deposition

## Electrochemical Testing

## Vapor Deposition

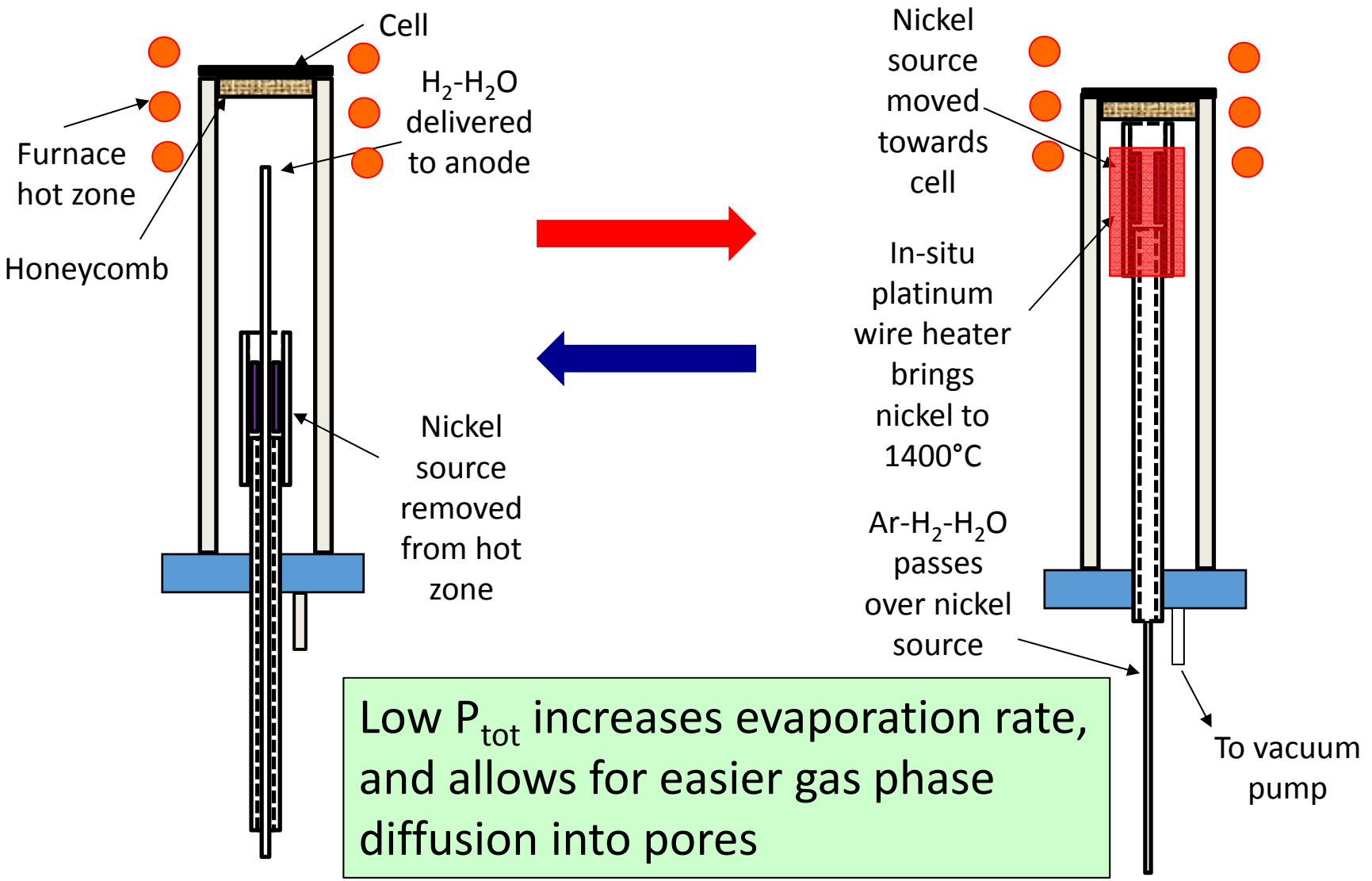


Low $P_{tot}$ increases evaporation rate, and allows for easier gas phase diffusion into pores

# Conclusions

- At high fuel utilization, the cell performance degrades due to increased anodic activation polarization losses
- Liquid infiltration of conventional Ni/YSZ anodes can more than double the TPB length of the cell
- This is expected to alleviate the increase of anodic activation polarization losses at high fuel utilization rates
- An innovative *in-situ* vapor-phase infiltration of the anode directly by Ni is proposed
- Process optimization can be achieved by manipulating the cell temperature, the water vapor content, the flow rate and the total pressure of the deposition chamber

# Future Work

- Optimization of vapor phase infiltration
- FIB-SEM based 3D-reconstruction of liquid infiltrated and vapor infiltrate cells
- Coarsening study on infiltrated cells
- Quantitative measurement of performance improvement at high fuel utilization conditions via cell modeling

# Acknowledgements

Project funding: DOE/SECA Award #: DE-FE0026096

A. Nikiforov, A. Krupp, D. Cetin, and R. Wang
*Boston University, Boston, MA 02215*

S. Markovich, H. Abernathy, S. Vora
*NETL, Pittsburgh, PA 15236*